H19 PTBP1 Figure S1

Diagram of feeding models

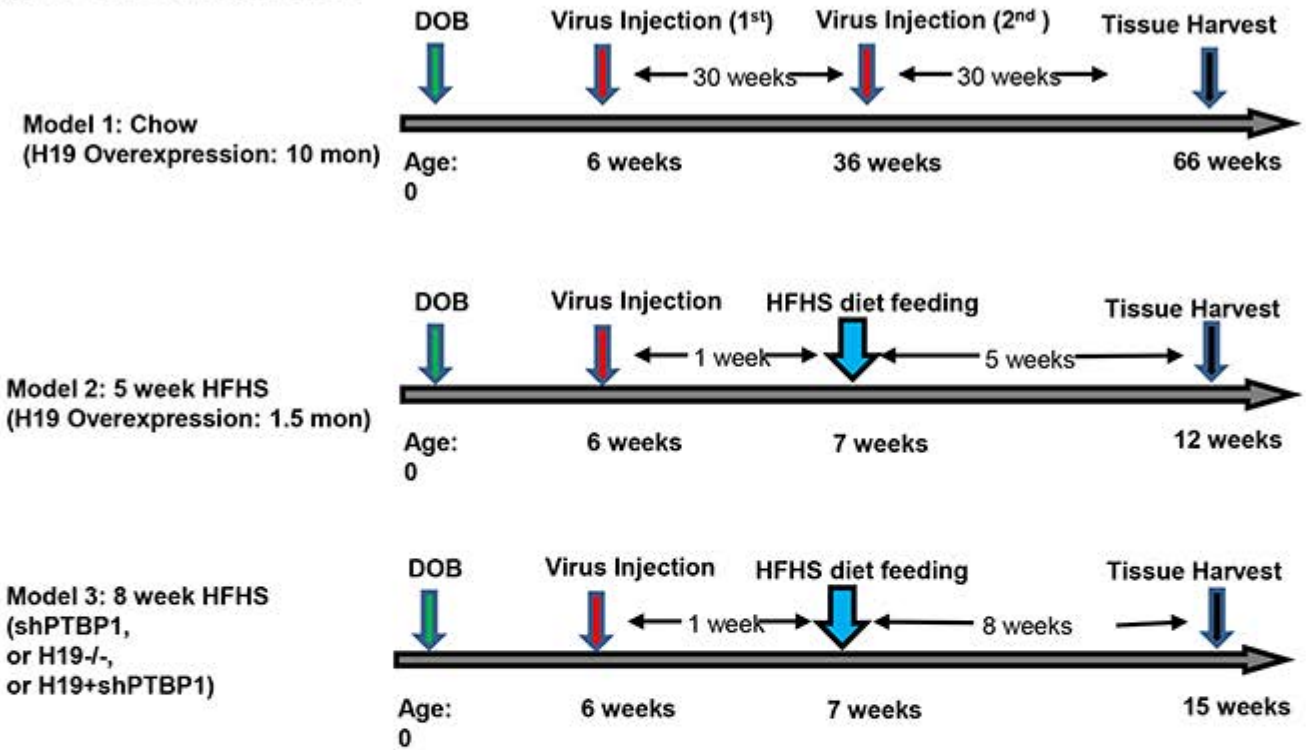

Virus particles:

AAV8-Null: $5x10^{10}$ viral particles/mouse
AAV8-H19: $5x10^{10}$ viral particles/mouse

Lenti-non target: $0.8x10^{8}$ viral particles/mouse
Lenti-ShPTBP1: $0.8x10^{8}$ viral particles/mouse

Fig. S1: Mouse models used for this study. The detailed timeline for AAV8-mediated H19 overexpression and lentivirus mediated PTBP1 knockdown is indicated. Red: The titers of viruses used for tail vein injection.

H19 PTBP1 Figure. S2

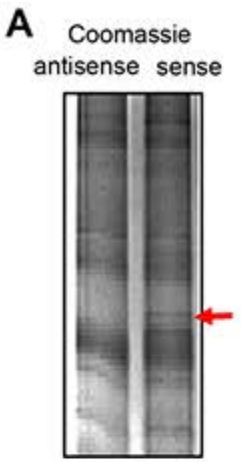

Score	Protein ID
1660	**PTBP1**
1140	SGPL1 (x)
828	MCCB (x)
791	SYFA
791	HNRPK (x)
755	NONO
729	LAP2B
715	YBOX1
623	SF3A3 (x)
558	DDX28
488	STAU1 (x)
481	YBOX3
378	PDIA1
363	PRS4
310	IFRD1

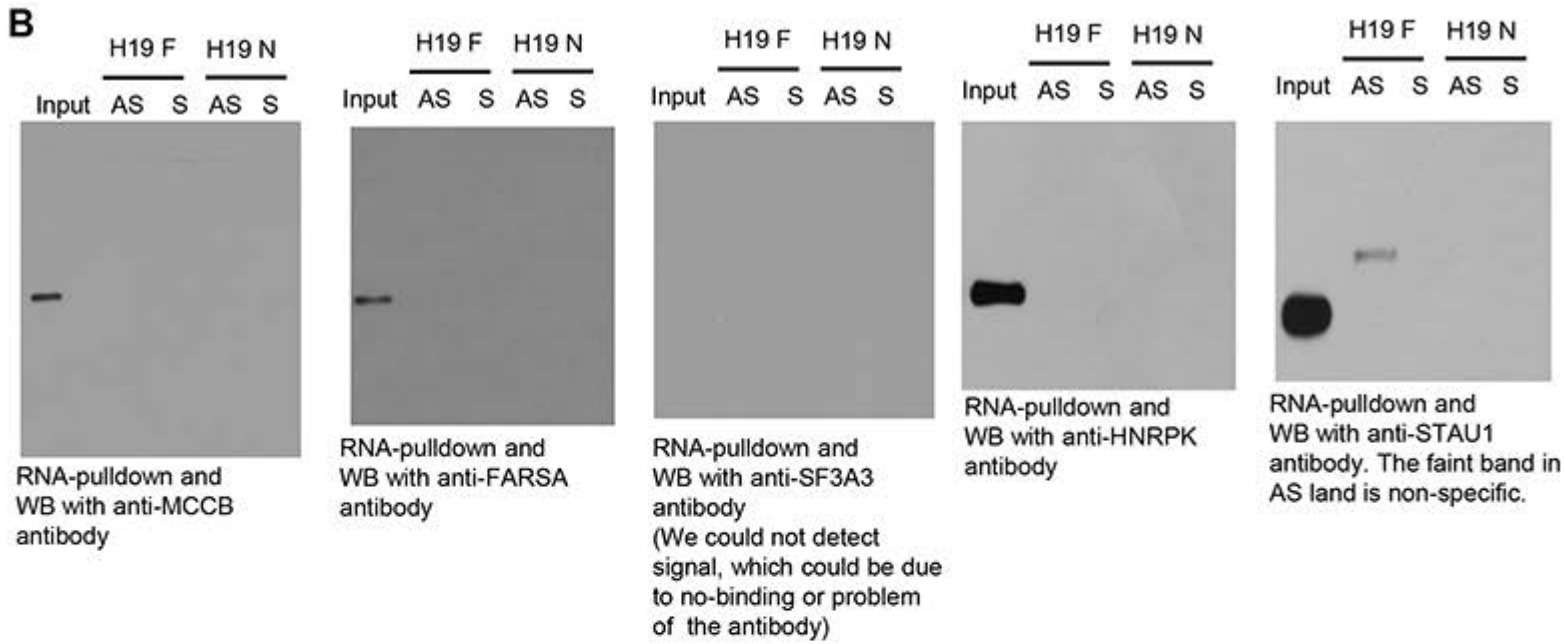

Fig. S2A: Coomassie blue gel indicating a unique band in H19 sense lane. See also main Fig. 1B.
Fig. S2B: Western blot to determine the specific interaction of sense *H19*RNA with its potential protein binding partners. See also main Fig. 1C. We tested six proteins and only PTBP1 was validated to bind H19RNA.

Fig. S3A: PTB binding sites within SREBP1c (Human)

General calculation parameters

Genome: Human (hg38)
Selected motifs: PTBP1(Hs/Mm):cucucu, PTBP1(Hs/Mm):ucuu
Stringency level: Medium
Conservation filter: Off

CDS

Results for sequence: SREBF1-003 cds:KNOWN_protein_coding
Genomic position: N/A (BLAT could not find at least 95% identity match for the sequence).
View binding sites predictions summary

Protein: PTBP1(Hs/Mm)

Position	Motif	Occurrence	Z-score	P-value
315	ucuu	gcucccaggcagcuugucuccaccuccugccacauugagcuccucucuugaag	2.134	1.64e-02
331	cucucu	gucuccaccuccugccacauugagcuccucucuugaagccuuccugagcgggccgc	2.259	1.19e-02
333	cucucu	cuccaccuccugccacauugagcuccucucuugaagccuuccugagcgggccgcag	2.955	1.56e-03
334	ucuu	uccaccuccugccacauugagcuccucucuugaagccuuccugagcgggccgca	2.134	1.64e-02
335	cucucu	ccaccuccugccacauugagcuccucucuugaagccuuccugagcgggccgcaggc	2.214	1.34e-02
336	ucuu	caccuccugccacauugagcuccucucuugaagccuuccugagcgggccgcagg	2.688	3.59e-03
344	ucuu	gccacauugagcuccucucuugaagccuuccugagcgggccgcaggcagcgccc	2.089	1.84e-02
345	cucucu	ccacauugagcuccucucuugaagccuuccugagcgggccgcaggcagcgcccuca	2.277	1.14e-02
347	ucuu	acauugagcuccucucuugaagccuuccugagcgggccgcaggcagcgcccuca	2.098	1.80e-02
430	cucucu	uccauugaagauguacccguccaugcccgcuuucucccccugggccugguaucaagg	1.884	2.98e-02
432	cucucu	cauugaagauguacccguccaugcccgcuuucucccccugggccugguaucaaggaa	1.884	2.98e-02
434	cucucu	uugaagauguacccguccaugcccgcuuucucccccugggccugguaucaaggaaga	2.250	1.22e-02
436	cucucu	gaagauguacccguccaugcccgcuuucucccccugggccugguaucaaggaagagu	1.884	2.98e-02
438	cucucu	agauguacccguccaugcccgcuuucucccccugggccugguaucaaggaagaguca	1.884	2.98e-02
591	cucucu	ccaccccuguguuaggcuaccccagcccucccgggaggcuucucuacaggaagcccu	1.884	2.98e-02
604	cucucu	aggcuaccccagcccucccgggaggcuucucuacaggaagcccucccgggaacaccc	2.250	1.22e-02
606	cucucu	gcuaccccagcccucccgggaggcuucucuacaggaagcccucccgggaacacccag	1.884	2.98e-02
618	cucucu	cuccgggaggcuucucuacaggaagcccucccgggaacacccagcagccgcugccu	1.884	2.98e-02
620	cucucu	ccgggaggcuucucuacaggaagcccucccgggaacacccagcagccgcugccugg	1.884	2.98e-02

Fig. S3A: PTB binding sites within SREBP1c (Human), continued

CDS

834	cucucu	ugcagccccacuucaucaaggcagacucgcugcuucugacagccaugaagacagac	1.929	2.69e-02
887	cucucu	gacggagccacugugaaggcggcaggucucagucccccuggucucuggcaccacugu	1.911	2.80e-02
889	cucucu	cggagccacugugaaggcggcaggucucagucccccuggucucuggcaccacugugc	1.911	2.80e-02
901	cucucu	gaaggcggcaggucucaguccccuggucucuggcaccacugugcagacagggccuu	2.259	1.19e-02
903	cucucu	aggcggcaggucucaguccccuggucucuggcaccacugugcagacagggccuuug	1.884	2.98e-02
912	cucucu	gucucaguccccuggucucuggcaccacugugcagacagggccuuugccgacccug	1.884	2.98e-02
959	ucuu	ccgacccuggugaguggcggaaccaucuuggcaacagucccacuggucguagau	2.161	1.53e-02
1175	ucuu	gaggcaaagcugaauaaaaucugcugucuugcgcaaggccaucgacuacauucgc	2.161	1.53e-02
1199	cucucu	gucuugcgcaaggccaucgacuacauucgcuuucugcaacacagcaaccagaaacu	1.741	4.08e-02
1201	cucucu	cuugcgcaaggccaucgacuacauucgcuuucugcaacacagcaaccagaaacuca	1.741	4.08e-02
1203	cucucu	ugcgcaaggccaucgacuacauucgcuuucugcaacacagcaaccagaaacucaag	2.107	1.76e-02
1252	cucucu	acucaagcaggagaaccuaagucugcgcacugcuguccacaaaagcaaaucucuga	1.839	3.30e-02
1259	cucucu	caggagaaccuaagucugcgcacugcuguccacaaaagcaaaucucugaaggaucu	1.839	3.30e-02
1275	cucucu	ugcgcacugcuguccacaaaagcaaaucucugaaggaucuggugucggccuguggc	2.214	1.34e-02
1277	cucucu	cgcacugcuguccacaaaagcaaaucucugaaggaucuggugucggccuguggcag	1.839	3.30e-02
1515	cucucu	gcaaggcaaagccagagcagcggccgucucugcacagccggggcaugcuggaccgc	1.839	3.30e-02
1568	ucuu	cgcucccgccuggcccugugcacgcucgucuuccucugccuguccugcaacccc	2.098	1.80e-02
1571	ucuu	ucccgccuggcccugugcacgcucgucuuccucugccuguccugcaaccccuug	2.688	3.59e-03
1574	ucuu	cgccuggcccugugcacgcucgucuucccucugccuguccugcaaccccuuggcc	2.134	1.64e-02
1577	ucuu	cuggcccugugcacgcucgucuuccucugccuguccugcaaccccuuggccucc	2.134	1.64e-02
1585	ucuu	gugcacgcucgucuuccucugccugucccugcaaccccuuggccuccuugcuggg	2.161	1.53e-02
1595	ucuu	gucuuccucugccuguccugcaaccccuuggccuccuugcuggggggcccggggg	2.152	1.57e-02

Fig. S3A: PTB binding sites within SREBP1c (Human), continued

				CDS
1763	ucuu	uggcugcucaaugggcuguuggugcucgucuccuuggugcuucucuuugucuac	2.161	1.53e-02
1765	cucucu	gcugcucaaugggcuguuggugcucgucuccuuggugcuucucuuugucuacggug	2.107	1.76e-02
1766	ucuu	cugcucaaugggcuguuggugcucgucuccuuggugcuucucuuugucuacggu	2.161	1.53e-02
1767	cucucu	ugcucaaugggcuguuggugcucgucuccuuggugcuucucuuugucuacggugag	2.107	1.76e-02
1768	ucuu	gcucaaugggcuguuggugcucgucuccuuggugcuucucuuugucuacgguga	2.161	1.53e-02
1769	ucuu	cucaaugggcuguuggugcucgucuccuuggugcuucucuuugucuacggugag	2.161	1.53e-02
1776	ucuu	ggcuguuggugcucgucuccuuggugcuucucuuugucuacggugagccaguca	2.161	1.53e-02
1778	cucucu	cuguuggugcucgucuccuuggugcuucucuuugucuacggugagccagucacacg	2.652	4.00e-03
1779	ucuu	uguuggugcucgucuccuuggugcuucucuuugucuacggugagccagucacac	2.161	1.53e-02
1780	cucucu	guuggugcucgucuccuuggugcuucucuuugucuacggugagccagucacacggc	2.652	4.00e-03
1781	ucuu	uuggugcucgucuccuuggugcuucucuugucuacggugagccagucacacgg	2.714	3.32e-03
1782	cucucu	uggugcucgucuccuuggugcuucucuuugucuacggugagccagucacacggccc	2.098	1.80e-02
1784	cucucu	gugcucgucuccuuggugcuucucuuugucuacggugagccagucacacggcccca	2.098	1.80e-02
1787	ucuu	cucgucuccuuggugcuucucuuugucuacggugagccagucacacggccccac	2.161	1.53e-02
2003	cucucu	aaccucauccgucaccugcugcagcgucucugggugggccgcuggcuggcaggccg	2.116	1.72e-02
2005	cucucu	ccucauccgucaccugcugcagcgucucuggguggggccgcuggcuggcaggccggg	1.741	4.08e-02
2019	cucucu	ugcugcagcgucucugggugggccgcuggcuggcaggccgggcaggggggccugcag	1.732	4.16e-02
2288	ucuu	agagugaagaccagucucccacgggccuugcauuuucugacacgcuucuuccug	2.152	1.57e-02
2295	ucuu	agaccagucucccacgggccuugcauuuucugacacgcuucuuccugagcagug	2.152	1.57e-02
2298	ucuu	ccagucucccacgggccuugcauuuucugacacgcuucuuccugagcagugccc	2.152	1.57e-02
2306	ucuu	ccacgggccuugcauuuucugacacgcuucuuccugagcagugcccgccaggcc	2.134	1.64e-02
2309	ucuu	cgggccuugcauuuucugacacgcuucuuccugagcagugcccgccaggccugc	2.688	3.59e-03

Fig. S3A: PTB binding sites within SREBP1c (Human), continued

CDS

2312	ucuu	gccuugcauuuucugacacgcuucuuccugagcagugcccgccaggccugccug	2.134	1.64e-02
2378	ucuu	ucagugccuccugccaugcaguggcucugccaccccgugggccaccguuucuuc	1.884	2.98e-02
2402	ucuu	cucugccaccccgugggccaccguucucuucguggaugggacuggcccgugcuc	2.446	7.22e-03
2501	ucuu	gacccccuggcccaggugacucagcuauuccgggaacaucucuuagagcgagca	1.884	2.98e-02
2513	cucucu	caggugacucagcuauuccgggaacaucucuuagagcgagcacugaacugugugac	2.116	1.72e-02
2514	ucuu	aggugacucagcuauuccgggaacaucucuuagagcgagcacugaacuguguga	1.884	2.98e-02
2515	cucucu	ggugacucagcuauuccgggaacaucucuuagagcgagcacugaacugugugaccc	1.741	4.08e-02
2516	ucuu	gugacucagcuauuccgggaacaucucuuagagcgagcacugaacugugugacc	2.446	7.22e-03
2535	cucucu	aacaucucuuagagcgagcacugaacugugugacccagcccaaccccagcccuggg	1.741	4.08e-02
2719	cucucu	cguagacccgguggccaaguggugggccucucugacagcuguggugauccacuggc	2.107	1.76e-02
2721	cucucu	uagacccgguggccaaguggugggccucucugacagcuguggugauccacuggcug	2.946	1.61e-03
2723	cucucu	gacccgguggccaaguggugggccucucugacagcuguggugauccacuggcugcg	2.205	1.37e-02
2745	cucucu	ccucucugacagcuguggugauccacuggcugcggcgggaugaggaggcggcugag	2.098	1.80e-02
3002	ucuu	agcuccauugacaaggccgugcagcuguuccugugugaccugcuucuuguggug	2.027	2.13e-02
3005	ucuu	uccauugacaaggccgugcagcuguuccugugugaccugcuucuuguggugcgc	2.027	2.13e-02
3018	ucuu	ccgugcagcuguuccugugugaccugcuucuuguggugcgcaccagccuguggc	2.027	2.13e-02
3021	ucuu	ugcagcuguuccugugugaccugcuucuugguggugcgcaccagccuguggcggc	2.580	4.94e-03

Fig. S3A: PTB binding sites within SREBP1c (Human) (Continued)

General calculation parameters

Genome: Human (hg38)
Selected motifs: PTBP1(Hs/Mm):cucucu, PTBP1(Hs/Mm):ucuu
Stringency level: Medium
Conservation filter: Off

3'UTR

Results for sequence: SREBF1-003 utr3:KNOWN_protein_coding
Genomic position: chr17:17812073-17812621 **Strand:** -

⊟ View binding sites predictions summary

Protein: PTBP1(Hs/Mm)

Position	Genomic coordinate	Motif	Occurrence	Z-score	P-value
25	chr17:17812597	cucucu	accccgugucccggccucagcaccccugucucuagccacuuuggucccgugcag	2.071	1.92e-02
27	chr17:17812595	cucucu	ccccgugucccggccucagcaccccugucucuagccacuuuggucccgugcagcu	2.625	4.33e-03
29	chr17:17812593	cucucu	ccgugucccggccucagcaccccugucucuagccacuuuggucccgugcagcuuc	2.625	4.33e-03
31	chr17:17812591	cucucu	gugucccggccucagcaccccugucucuagccacuuuggucccgugcagcuucug	2.071	1.92e-02
38	chr17:17812584	cucucu	cggccucagcaccccugucucuagccacuuuggucccgugcagcuucuguccugcg	2.107	1.76e-02
373	chr17:17812249	cucucu	cuuggcuuucccggacugcaagcaggggcucugccccagaggccucucucuccgucg	2.759	2.90e-03
375	chr17:17812247	cucucu	uggcuuucccggacugcaagcagggcucugccccagaggccucucucuccgucgug	2.759	2.90e-03
377	chr17:17812245	cucucu	gcuuucccggacugcaagcagggcucugccccagaggccucucucuccgucguggg	2.018	2.18e-02
388	chr17:17812234	cucucu	cugcaagcagggcucugccccagaggccucucucuccgucgugggagagagacgug	2.750	2.98e-03
390	chr17:17812232	cucucu	gcaagcagggcucugccccagaggccucucucuccgucgugggagagagacgugua	3.955	3.83e-05
392	chr17:17812230	cucucu	aagcagggcucugccccagaggccucucucuccgucgugggagagagacguguaca	3.955	3.83e-05
394	chr17:17812228	cucucu	gcagggcucugccccagaggccucucucuccgucgugggagagagacguguacaua	3.402	3.34e-04
396	chr17:17812226	cucucu	agggcucugccccagaggccucucucuccgucgugggagagagacguguacauagu	2.750	2.98e-03
398	chr17:17812224	cucucu	ggcucugccccagaggccucucucuccgucgugggagagagacguguacauagugu	2.009	2.23e-02
537	chr17:17812085	ucuu	uuguacagagaauuaaaaaugaaauuauuuauaaucug	2.027	2.13e-02
546	chr17:17812076	ucuu	gaauuaaaaaugaaauuauuuauaaucug	2.027	2.13e-02

H19 PTBP1 Figure. S3B-S3E

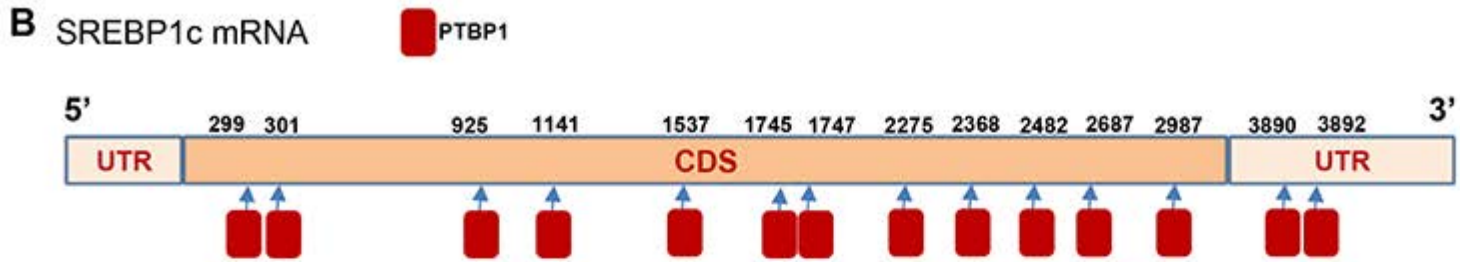

Fig. S3B: Diagram showing PTB binding sites within SREBP1c mRNA

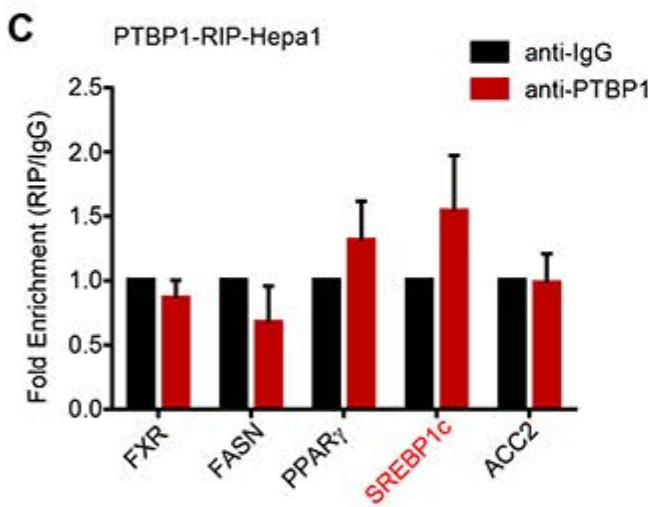

Fig. S3C: RNA IP to determine whether PTBP1 interacts with FXR, FASN, PPARγ, SREBP1c and ACC2 mRNAs (endogenous).

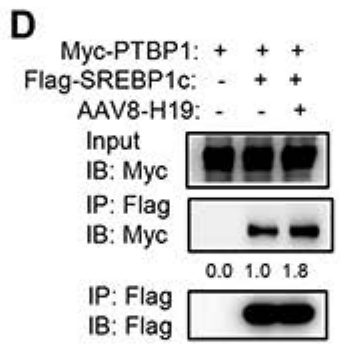

This is a repeating experiment of Figure 1B

Fig. S3D: Co-IP followed by Western blot to determine PTBP1 and SREBP1c protein interaction. See also main Fig. 1B.

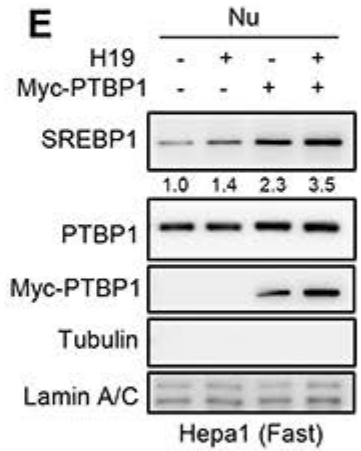

This is a repeating experiment of Figure 1C.

Fig. S3E: Western blot to determine the effect of H19 and PTBP1 on static levels of SREBP-1 protein. See also main Fig. 1C.

H19 PTBP1 Figure. S4

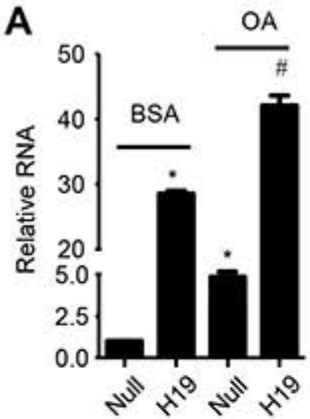

Fig. S4A: qPCR of H19RNA expression in hepatocytes treated with oleic acid. Cells were transduced with AAV8-control null or AAV8-H19 virus in the presence or absence of oleic acid (OA, 200 μM, 16 hr). *p<0.05 vs Null BSA; #p<0.05 vs H19 BSA and Null OA.

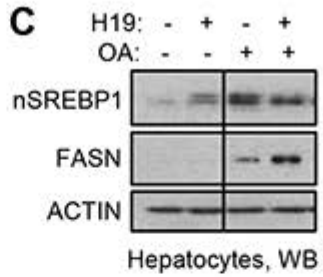

Fig. S4C: WB of protein expression in primery hepatocytes treated with OA in the presence or absence of H19

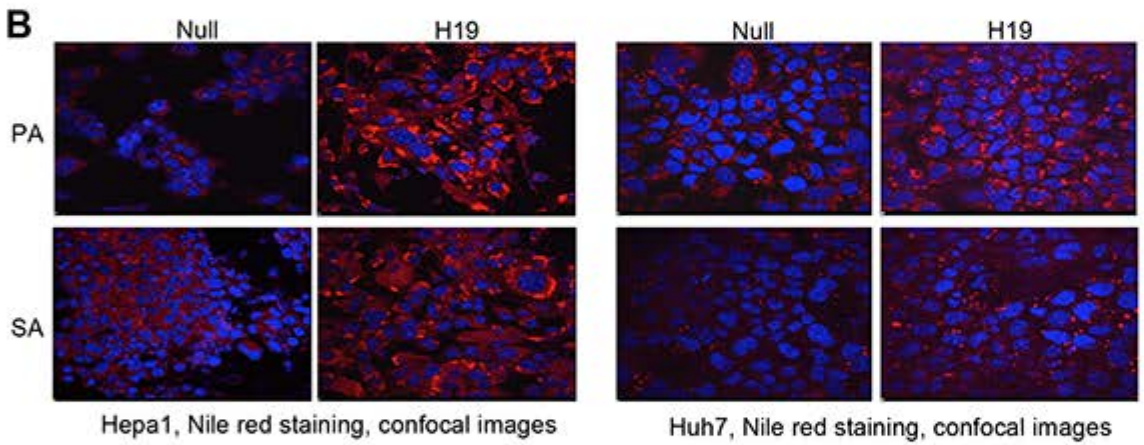

Fig. S4B: Confocal images of Nile red staining of neutral lipid in Hepa1 and Huh7 cells. Cells were transduced with AAV8-Null or AAV8-H19 virus in the presence or absence of palmitic acid (OA) or stearic acid (SA).

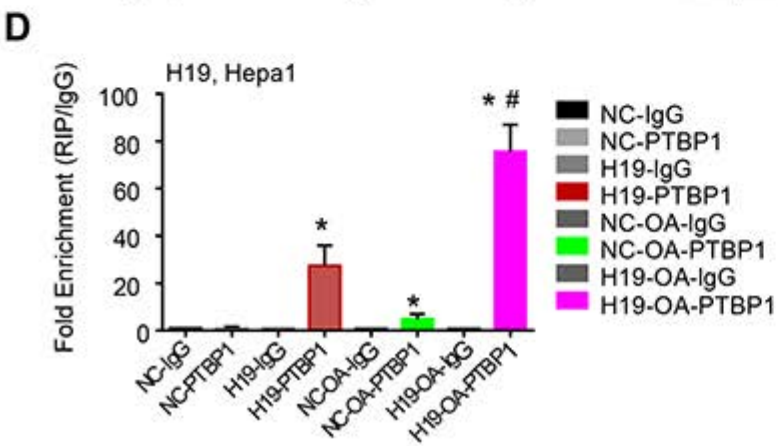

Fig. S4D: PTBP1 and H19 endogenous interaction in Hepa-1 cells. RNA immunoprecipitation (RIP) to detect the association of H19 and PTBP1 in Hepa1 cells treated with DMSO or OA for 24 hr.

H19 PTBP1 Figure. S5

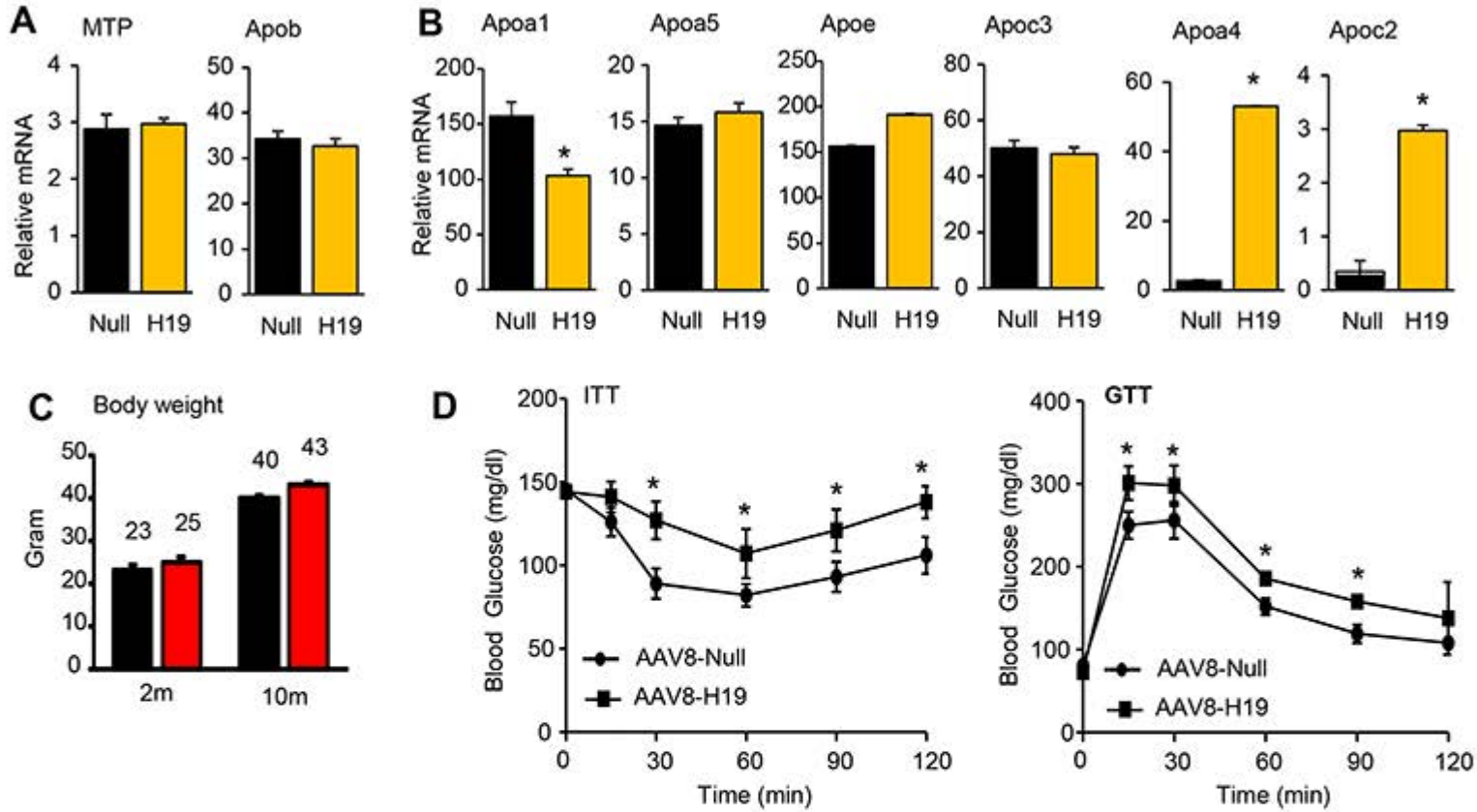

Fig. S5A-S5B: qPCR of gene expression in Null and H19 mice.
Fig. S5C: Body weight of Null and H19 mice at 2 month or 10 month after AAV8-virus transduction.
Fig. S5D: Insulin tolerance test (ITT) was performed after a 4 hr fast by an intraperitoneal injection of insulin at a dose of 2U/kb body weight. Glucose tolerance test (GTT) was performed in mice after an overnight fast by an intraperitoneal injection of glucose at a dose of 2 g/kb body weight. Blood was drawn from the tail vein at 0, 15, 30, 60, 90, and 120 minutes and glucose levels were measured using a glucometer (n=5-10 mice/group). Data are shown as mean ± SEM, *P<0.05 H19 vs Null.
The same mice as in Fig. 4C-4F.

H19 PTBP1 Figure. S6

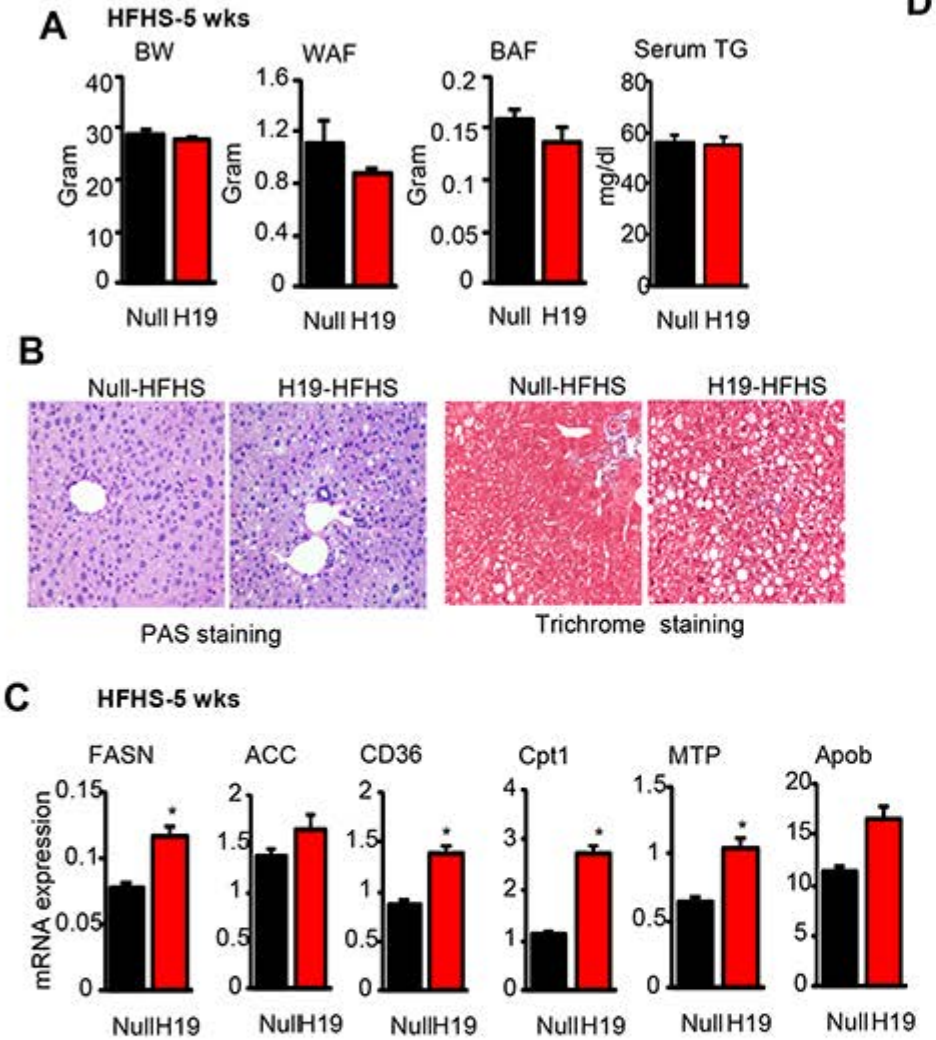

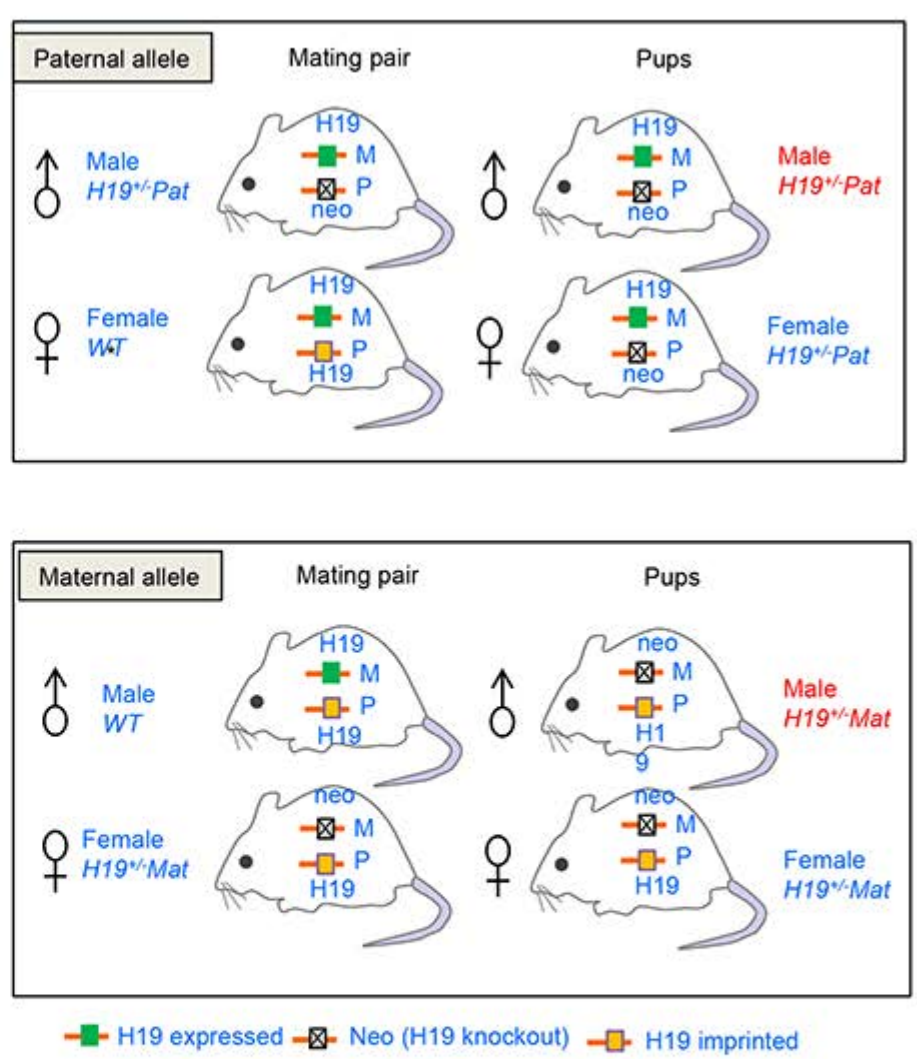

Fig. S6A: Body weight, WAF and BAF weights, and serum TG levels of Null and H19 mice under a HFHS diet for 5 weeks.
Fig. S6B: PAS and Trichrome staining of liver sections in Null and H19 mice under a HFHS diet for 5 wks.
Fig. S6C: qPCR of gene expression in Null and H19 mice under a HFHS diet for 5 wks.
Fig. S6D: Mating scheme to generate H19 knockout mice. Mice with H19 deleted from the paternal allele were used as control and mice with H19 deleted from maternal allele were H19-/-.
The same mice as in Fig. 5A-5C.

H19 PTBP1 Figure. S7

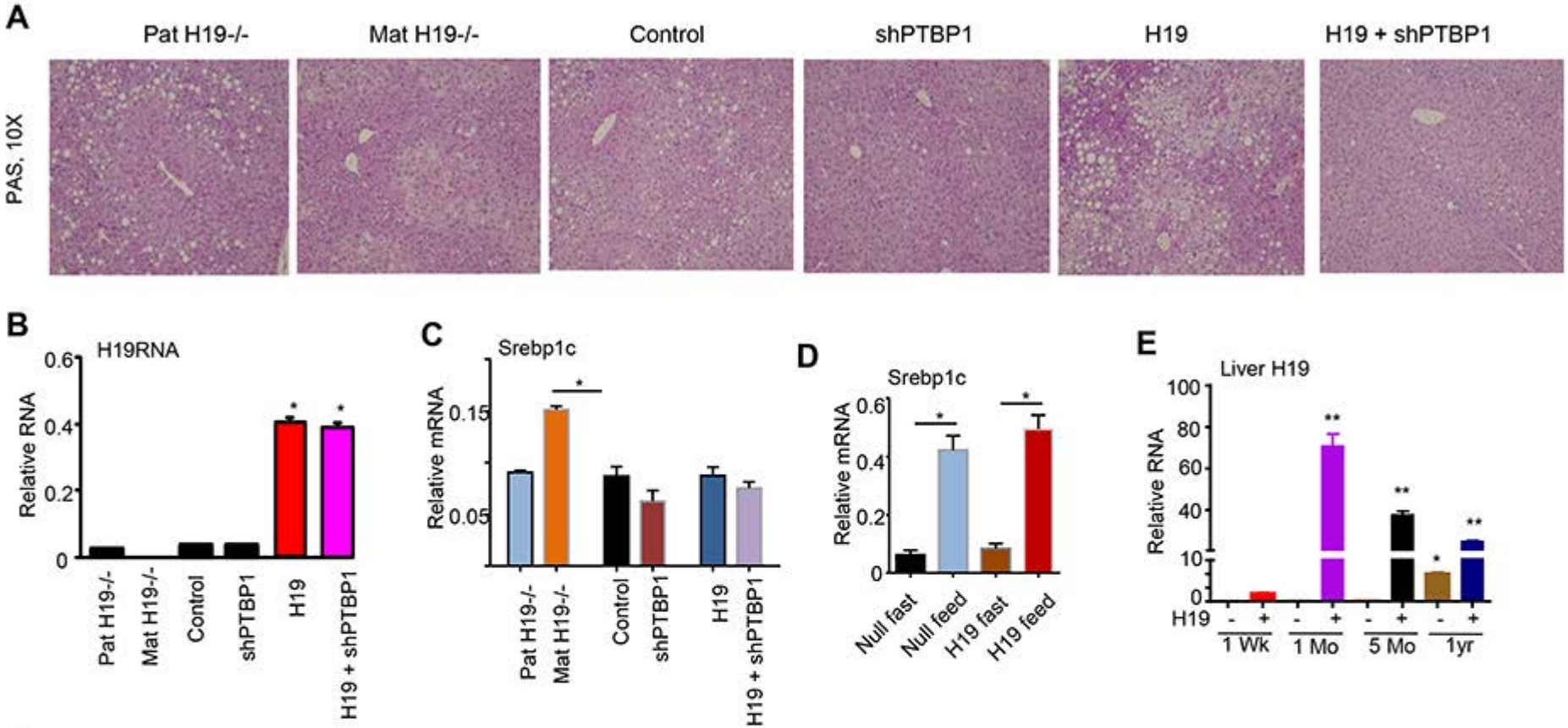

Fig. S7A: PAS staining of liver sections in Pat H19-/- and Mat H19-/-; control and shPTBP1; H19 and H19+shPTBP1 mice under a HFHS diet for 8 weeks. The same mice as in Fig. 5D-5F.
Fig. S7B-S7C: qPCR of H19RNA and Srebp1c mRNA. The same mice as in Fig. 5D-5F.
Fig. S7D: qPCR of Srebp1c mRNA in Null-HFHS and H19-HFHS mice under fasting and feeding conditions. The same mice as in Fig. 6A.
Fig. S7E: qPCR of H19RNA in AAV8-control or AAV8-H19 mice during the course of two years. H19RNA maintained at constant levels from 5 months to 1 year.
Fig. S7F: qPCR of H19RNA in extra-hepatic tissues in AAV8-control or AAV8-H19 mice one year after virus injection.

H19 PTBP1 Figure. S8

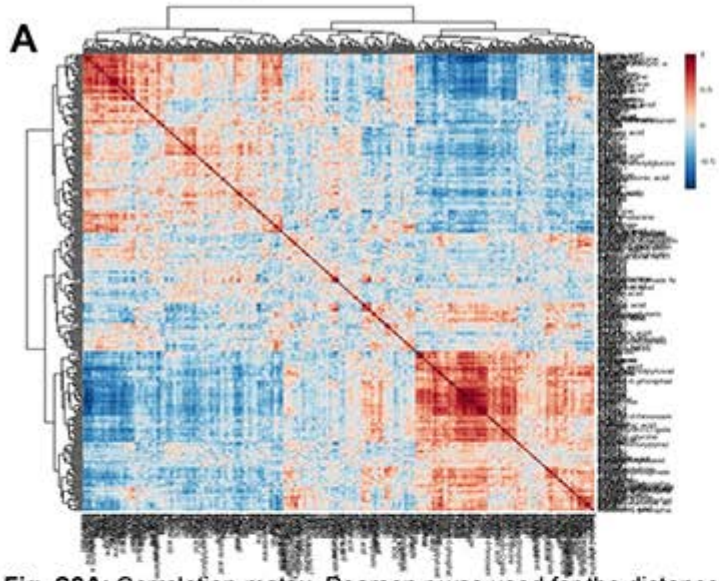

Fig. S8A: Correlation matrix. Pearson r was used for the distance measure. Correlation matrix showing correlation coefficients. Positive correlations are displayed in red and negative correlations in blue color. Color intensity and the size of the circle are proportional to the correlation coefficients

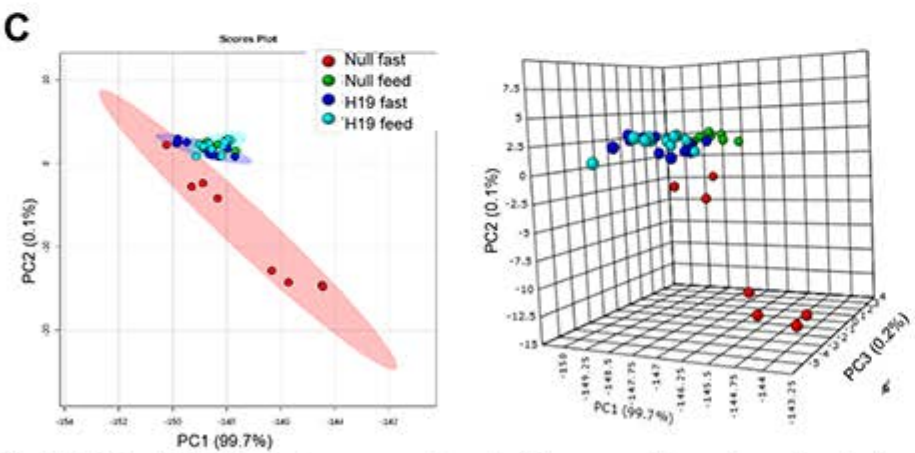

Fig. S8C: The PCA (principal component analysis) scores plots performed using two (left) or three (right) principal components corresponding to data obtained from Null-fast, Null-feed, H19-fast, and H19-feed mice. Each point summarizes all the information provided by the four different analytical conditions (145 identified metabolites). The ovals filled with different color donate 95% confidence interval Hotelling's ellipses. The PCA scores plots showed an almost complete separation between control-fast and other three groups.

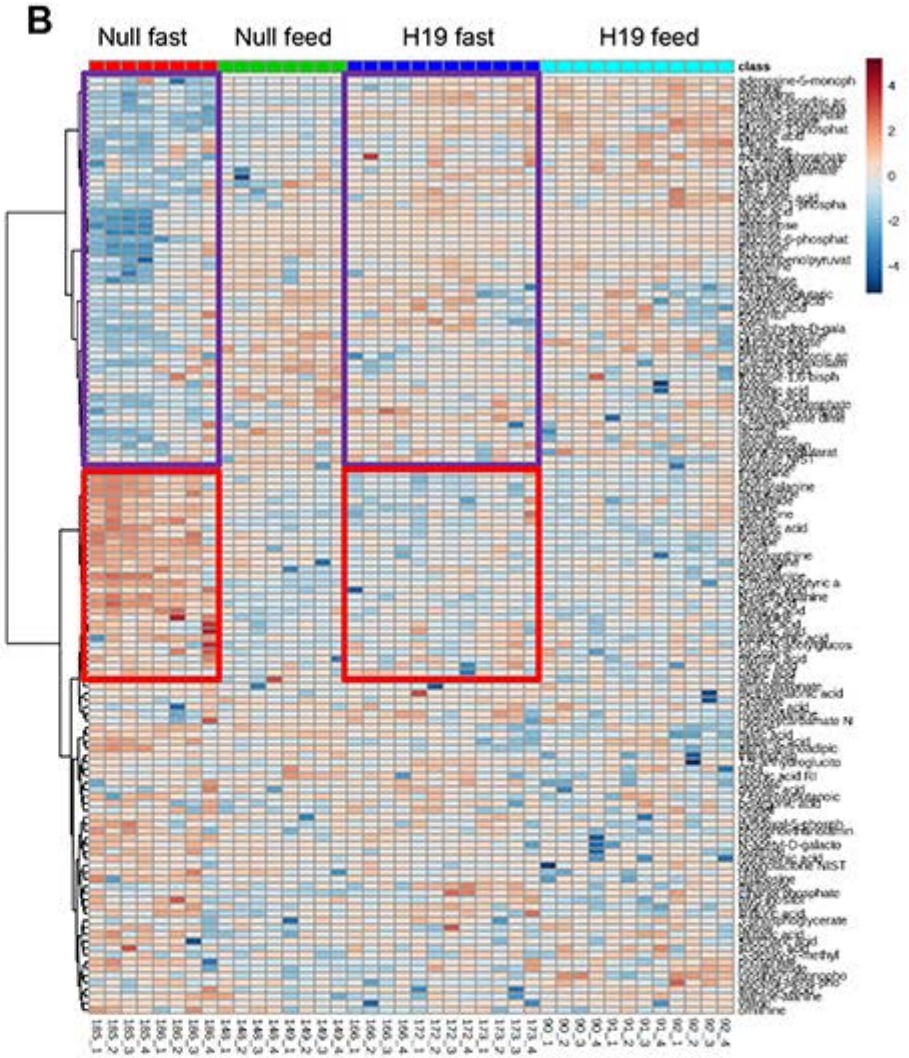

Fig. S8B: Heatmap showing clustered metabolites in indicated groups. Each column represents a sample, and each row represents a metabolite. Orange indicates above-mean intensity, blue denotes below-mean intensity, and the degree of color saturation reflects the magnitude of intensity relative to the mean. Heatmap was generated by MetaboAnalyst 3.0 using log2 fold changes. Fasting causes significant changes in metabolites profiles relative to feeding in control null mice. However, such changes were blunted in H19-fast group. Each lane represents an individual sample. Purple box: metabolites levels decreased by fasting in Null-fast vs Null-feed, but not in H19-fast; red box: metabolites levels increased by fasting in Null-fast vs Null-feed, but not in H19-fast.

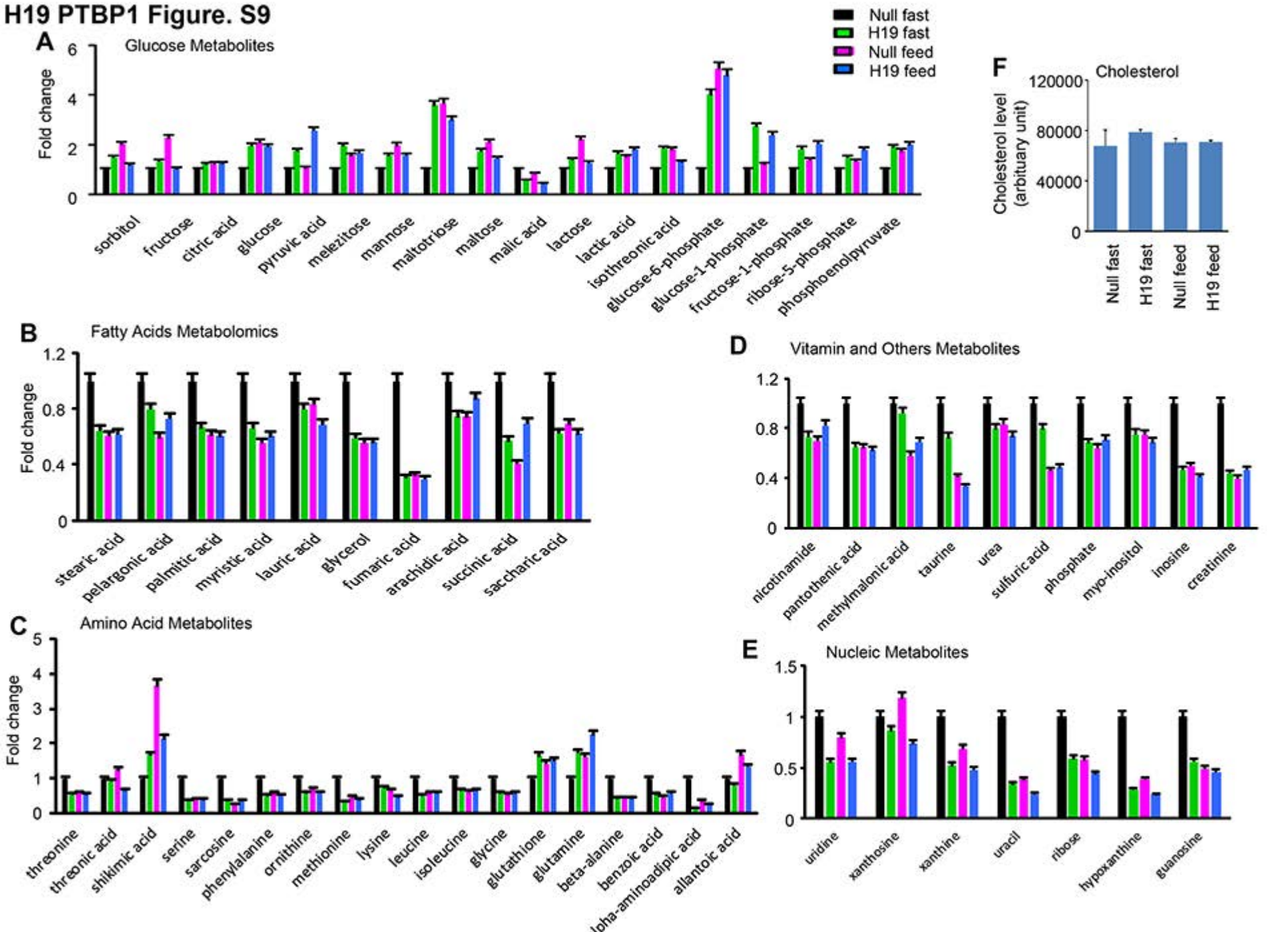

Fig. S9: Major metabolites altered by fasting or by H19. Null fast: set as 1.

H19 PTBP1 Figure. S10

A

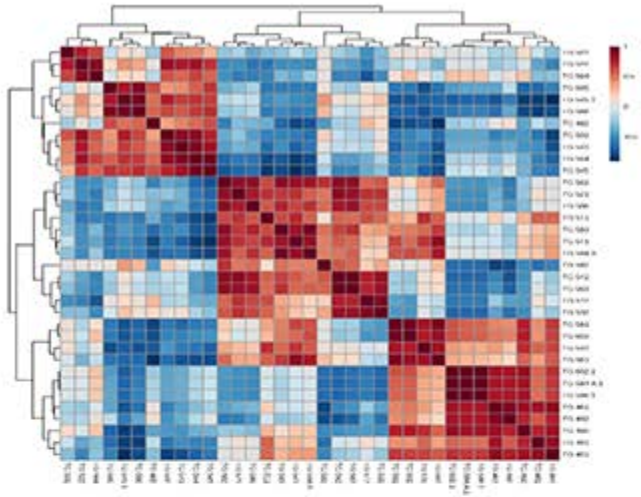

Fig. S10A: Correlation matrix showing correlation coefficients for triglyceride (TG) lipid species under fasting conditions only. Pearson r was used for the distance measure. Positive correlations are displayed in red and negative correlations in blue. Color intensity are proportional to the correlation coefficients.

B

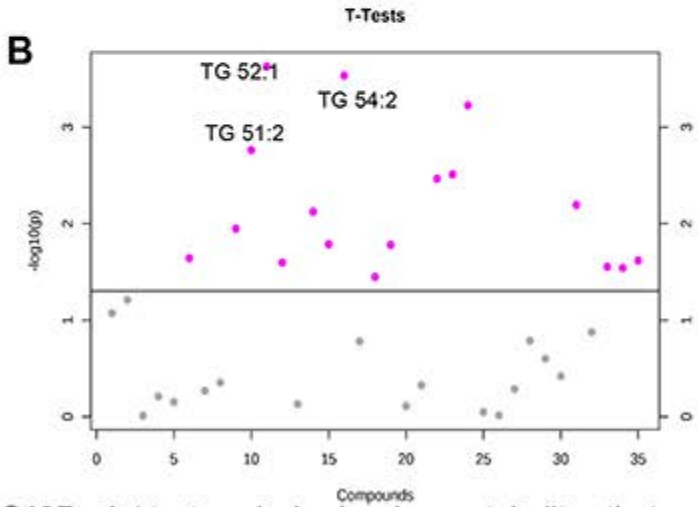

Fig. S10B: A *t*-test analysis showing metabolites that are significantly altered between Null and H19 mice. Each dot represents a metabolite plotted as a compound number (x-axis) and statistical significance (−log 10 (p-value), y-axis).

C

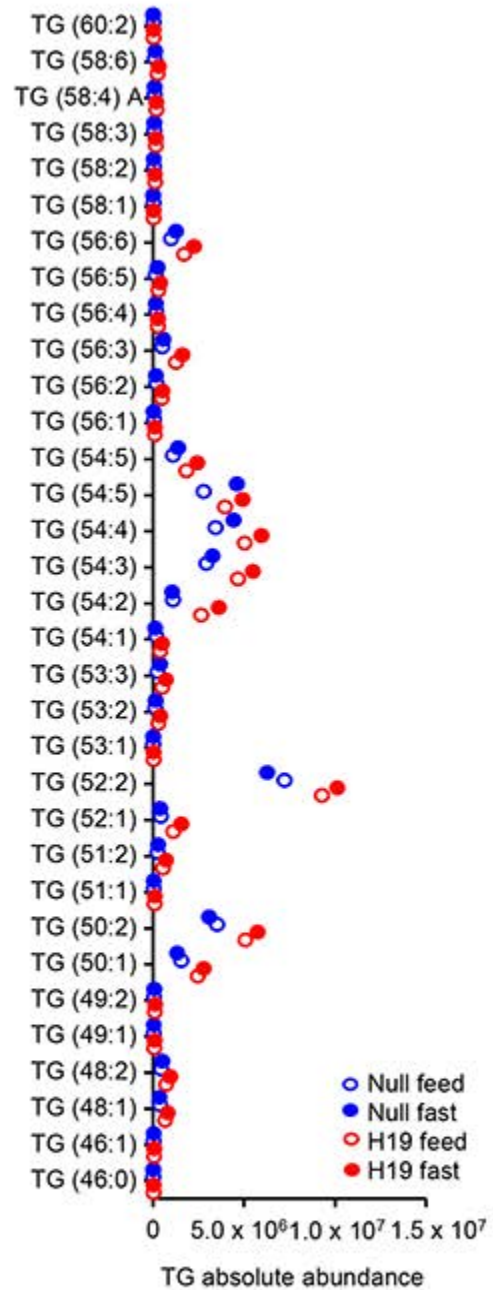

Fig. S10C: TG lipid species are expressed as absolute abundance according to TG chain length (top to bottom).

H19 PTBP1 Figure. S11

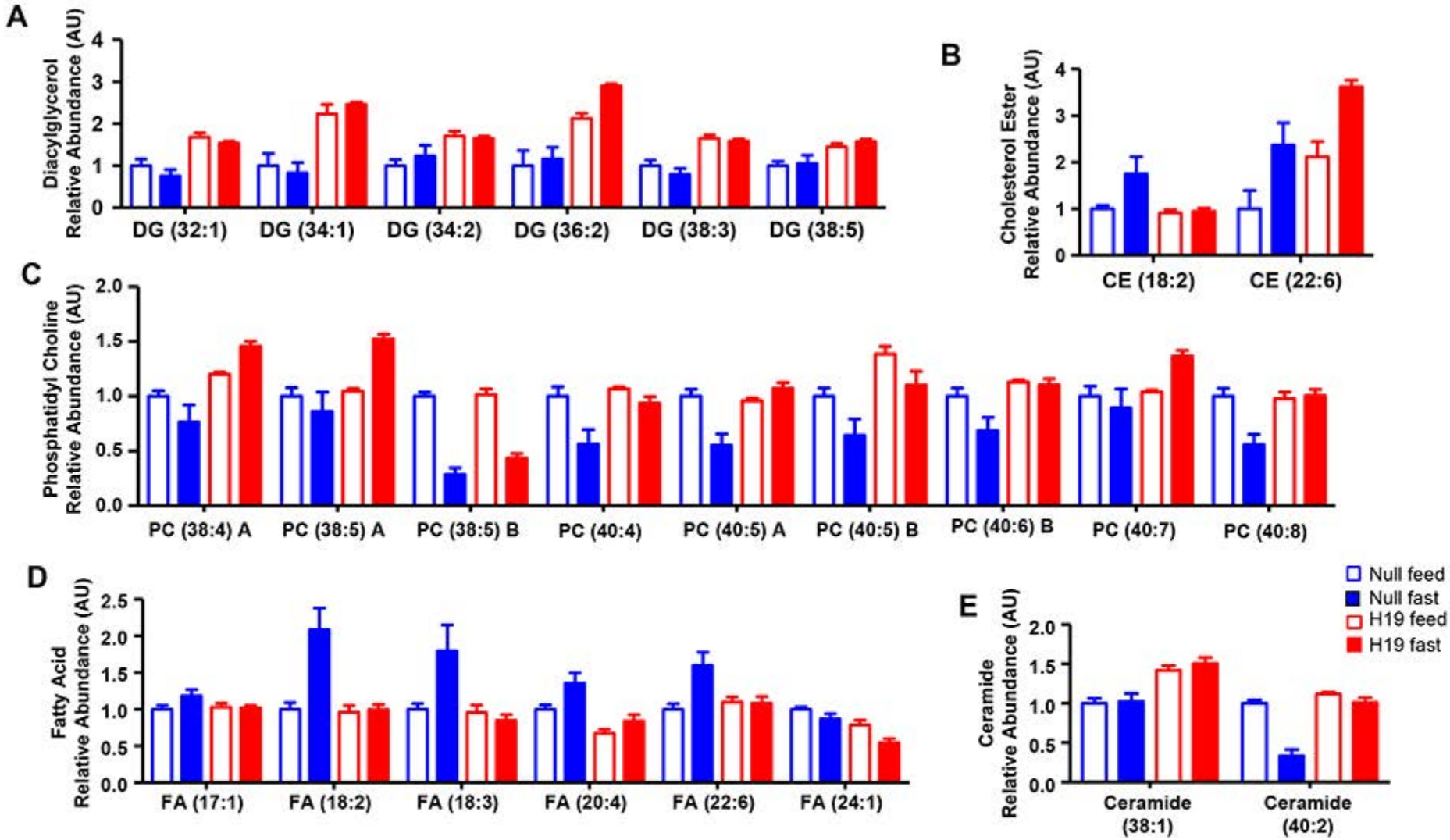

Fig. S11: Other lipid metabolites altered by fasting or by H19. Null feed: set as 1.

lncRNA H19 Interacts with Polypyrimidine Tract-Binding Protein 1 to Reprogram Hepatic Lipid Homeostasis

Chune Liu, Zhihong Yang, Jianguo Wu, Li Zhang, Sangmin Lee, Dong-Ju Shin, Melanie Tran, Li Wang

Supplemental Experimental Procedures

Mouse Experiments

Wild-type C57BL/6J (Jackson Laboratory) and *H19*$^{-/-}$ mice (Venkatraman et al., 2013) were handled in accordance with guidelines from the Institutional Animal Care and Use Committee (IACUC). Because H19 is a paternal imprinted gene, maternal *H19*-deleted mice were used for experiments of H19 knockout (Mat *H19*$^{-/-}$) and paternal *H19*-deleted mice (Pat *H19*$^{-/-}$) were used as wild type controls. Five of randomized male mice (6 wks) of each group were injected via tail vein with purified adeno-associated viral vector serotype 8 (AAV8) viruses or lenti-viruses containing a liver-specific thyroxine-binding globulin (TBG) promoter driving H19 gene overexpression or Ptbp1 knockdown. Mice were fed a standard chow (Harlan Teklad, TD.2018 Teklad Global 18% Protein Rodent Diet) or a HFHS diet (Harlan Teklad, TD.08811 44.6%kcal Fat Diet (21% anhydrous milk fat, 2% soybean oil, 40.6% kcal carbohydrate and 14.8% kcal protein) (also see Supplemental Information and Supplementary Figure 1 for detailed experimental models and conditions). All samples were analyzed under fasting conditions unless otherwise indicated. Basic procedures to analyze animal metabolic phenotypes and serum parameters were described previously (Tabbi-Anneni et al., 2010). Metabolomics and lipidomics analyses were carried out at the UC Davis Metabolomics Center. Protocols for animal use were approved by IACUC at the University of Connecticut. The coded human liver specimens were obtained through the Liver Tissue Cell Distribution System (Minneapolis, Minnesota), which was funded by NIH Contract # HSN276201200017C.

RNA Pull-down and Mass Spectrometry

RNA pull-down was performed according to a method described previously (Tsai et al., 2010). To prepare a plasmid construct as a template for RNA synthesis, H19 RNA was amplified by PCR and cloned into a pGEM-T Easy (Promega) cloning vector. Biotin-labeled RNA probes were prepared using *in vitro* transcription of appropriately linearized plasmid templates with biotin RNA labelling mix (Roche) and T7 or SP6 RNA polymerase, treated with RNase-free DNase I (Roche), and purified with the RNeasy Mini Kit (Qiagen). Aliquots of 2 μg of biotinylated RNAs were used for pull-down experiments. Total protein extracts were obtained from Hepa-1 cells with NP-40 buffer (1% NP-40, 150 mM NaCl, 50 mM Tris-Cl, pH 8.0, 0.5 mM DTT, 1 mM PMSF). Extracts containing 1 mg of protein were precleared with streptavidin magnetic beads (Promega) and then incubated with 2 μg of biotinylated RNA for 2 h at 4 °C. The bound proteins were recovered by further incubating with 20 μl of streptavidin magnetic beads for 1 h at 4 °C. Beads were washed briefly five times with washing buffer (10 mM Tris–HCl, 1 mM EDTA, and 2 m NaCl), boiled in SDS–PAGE sample buffer. RNA-associated proteins were eluted and resolved by SDS–PAGE followed by Coomassie staining. The SDS-PAGE-separated band unique for *H19* sense RNA was excised and in-gel digested with trypsin for mass spectrometry (LC-MS) analysis at the Yale Keck Proteomics Center. Primers containing T7 or T3 promoter sequences used for synthesizing biotin-labelled H19 full length, H19 5'end, and also negative antisense RNA (complementary to sense RNA) are listed in Supplementary Table S1. Cytoplasmic and nuclear fractions from cultured cells or frozen liver tissues were extracted as

described (Zhou et al., 2010). Western blot analysis (Yang et al., 2013) with RIP pulled-down lysates was used to validate H19 interaction proteins.

RNA immunoprecipitation (RIP)
RIP was performed as described in our previous protocol with slight modifications(Zhang et al., 2017). Cells (3×10^6) were UV–cross-linked at 254 nm (2000 J/m^2), followed by incubation within 200 μL of lysis solution [0.5% NP40, 0.5% $C_{24}H_{39}O_4Na$, 200 U/mL RNase inhibitor (Promega), and protein inhibitor (Roche, Penzberg, Germany)] for 25 minutes with vigorous shaking. An anti-PTBP1 antibody or mouse immunoglobulin G (IgG) (Sigma) was added into the whole cell lysate for 1-2 hours on ice with gentle shaking. Antibody/Protein/RNA complexes were recruited using 30 μL of protein A/G agarose beads (Sigma). RNAs associated with PTBP1 were recovered with Trizol-chloroform and analyzed by RT-PCR or qPCR.

Primary Hepatocyte Isolation and in vitro Transduction
Hepatocytes were isolated from 5 individual wild type or 5 individual H19 overexpressed mice as previously described (Zhang et al., 2014). Briefly, the mice were anesthetized with Ketamine HCl 100mg/kg and Xylazine HCl 10mg/kg by i.p. injection and the abdomen was opened surgically. The liver was first perfused with 50 ml of Solution I (9.5 g/l Hank's balanced salt solution, 0.5 mmol/l EGTA, pH 7.2) and then perfused with 50 ml of Solution II (9.5 g/l Hank's balanced salt solution, 0.14 g/l collagenase IV, and 40 mg/l trypsin inhibitor, pH 7.5). After perfusion, the liver was transfered into a sterile petri dish and cells were dissociated with forceps up and down gently, then filtered through the 75μm pore mesh. The hepatocytes were then suspended in 50% percoll (Sigma), collected by centrifugation, and seeded onto collagen-coated culture plates in William E medium (Sigma). After a 4-hour incubation, the medium was replaced with William E fasting medium. On the second day, hepatocytes were infected with $5x10^{10}$ genome copies (GC) of AAV8-H19 or AAV8-Null. At 24 hour post-infection, the hepatocytes underwent specific treatments as indicated in figure legends.

Cell Lines and in vitro Transfection
Human hepatocellular carcinoma (HCC) cell line Huh7, and mouse hepatocellular carcinoma (HCC) Hepa1 were purchased from ATCC in 2010 and were made aliquots and stored in a liquid nitrogen immediately after the first passage. All cell lines were last confirmed by short tandem repeat analysis of cellular DNA (PowerPlex1.2Kit; Promega) in 2015. When cells were recovered from liquid nitrogen in 2015 they were found to be free of mycoplasma (e-Myco Kit; Boca Scientific). The cell lines were passaged for less than 6 months when used for experiments. Huh7 and Hepa1 cells were maintained in DMEM supplemented with 10% fetal bovine serum (FBS), 100 IU/ml penicillin G, and 100 μg/ml streptomycin (Invitrogen, NY, USA), 1 mM HEPES, 1 mM sodium pyruvate, 2 mM L-glutamine. Plasmids including Flag-SREBP1c and Myc-PTBP1 were transfected in vitro by X-tremeGENE HP DNA Transfection Reagent (Roche) as previously described (Zhang et al., 2016; Zhang et al., 2014). For luciferase reporter assay, Hepa1 cells were transiently transfected with a vector containing sterol response elements (SRE) ligated to a luciferase reporter in combination with a vector for SREBP1c in the presence or absence or PTBP1 or H19 co-expression. The luciferase activity was normalized to β-gal activity.

Histology Analysis
Liver tissues were fixed in formalin on shaking device for 48 hours, paraffin embedded and then sliced into 5μm sections before subjecting to H&E staining, Periodic Acid-Schiff (PAS) staining and Trichrome Masson staining according to standard protocols. For the Oil Red O staining, 5μm frozen sections from snap-frozen liver tissues were fixed in 10% formalin for 30 min, stained in 0.5% Oil Red O in isopropanol for 15 min, and then in hematoxylin for the counter

staining of nuclei for 2 min. Nile red staining of cultured cells was performed to check intracellular neutral lipid accumulation as described (Wu et al., 2015). Digital images were captured under Fluorescent microscope (Olympus) or confocal microscope (Leica SP8). Eight randomly selected fields for each slide were analyzed with Image J. For quantification of Nile Red staining, eight Images were randomly chosen and submitted to Image J (version 2.0.0-rc-43/1.50g) analysis. Positive areas were selected, and the relative intensity was calculated and compared with the control group.

Western Blotting

Protein lysates (30 μg) were resolved by SDS-PAGE and transferred to polyvinylidene fluoride membrane. Membranes were blocked, incubated with primary antibodies at 4^{o}C overnight followed by horseradish peroxidase-conjugated corresponding secondary antibody incubation. Antibody binding was visualized with ECL substrate (Thermo Fisher Scientific, #34080) according to the manufacturer's protocol. The following antibodies were used at a dilution of 1:1,000: p-AKT (#4060), AKT (#9272), p-ERK (#4695), ERK (#9102), p-JNK (#9251), JNK (#9252) myc-tag (#2276), α-Tubulin (#2125), and Lamin A/C (#4777) were from Cell Signaling Technology; antibodies against PPARα (sc-9000), PPARγ (sc-7273), FASN (sc-20140), ACC (sc-30212), MCCB (sc-366942), STAU1 (sc-377484) and ACTIN (sc-47778 HRP) were purchased from Santa Cruz Biotechnology; antibodies against PTBP1 (ab83897), SF3A3 (ab176581) and HNRPK (ab32969) were purchased from Abcam; antibodies against SREBP1 (MA5-16124) and FARSA (PA5-51657) were purchased from Thermo Fisher Scientific; antibodies against PTBP1 were kindly provided by Dr. Douglas L. Black (UCLA Brain Research Institute); HRP-conjugated anti-mouse and anti-rabbit secondary antibodies were purchased from Thermo Fisher Scientific. HRP-conjugated FLAG antibody was purchased from Sigma. An antibody for SGPL1 (AF5535-SP) was purchased from R&D systems. For WB analysis, equal amounts of protein from five livers in each group (n=5/group) were pooled, and single or duplicate loading was used.

RNA Isolation and Real-time qPCR

Total mRNA was isolated from frozen livers using TRIzol (Invitrogen) according to the manufacturers' instructions. RNA was quantified by NanoDrop 2000 Spectrophotometer (Thermo Scientific). Complementary DNA was synthesized from total RNA using iScript cDNA Synthesis Kit (BIO RAD). Quantitative RT-PCR using the SYBR Green Dye-based assay was performed on CFX384 Real-Time PCR System (BIO RAD). Data were normalized to hprt1 or 18S or to control samples.

Hepatic Lipid Extraction and Blood Chemistry

Liver tissues and plasma samples were isolated from mice that had received a normal chow diet or a HFHS diet or that had been fasted as indicated. To determine hepatic triglyceride levels, approximately 200 mg of liver tissue was homogenized in chloroform/methanol followed by centrifugation. The lower chloroform phase was collected and evaporated under vacuum, and the residual lipids were resuspended with 10% Triton X-100. Triglyceride levels and free fatty acid levels were measured using commercial kits (BioAssay Systems). Hepatic triglyceride levels were determined by normalization to the mass of liver tissue used for measurement of triglyceride levels. Plasma samples were subjected to analysis for quantitation of triglyceride and free fatty acid levels using commercial kits (BioAssay Systems). Alanine transaminase (ALT) and Aspartate aminotransferase (AST) were measured by Infinity ALT (GPT) Liquid Stable Reagent and AST (GOT) Liquid Stable Reagent according to the manufacturer’s instructions (Thermo Scientific). GTT and ITT were performed as previously described (Huang et al., 2007).

Protein Extraction and Fractionation

Whole liver protein lysates were extracted with RIPA buffer supplemented with protease and phosphatase inhibitors. Cytoplasmic and nuclear fractions from cultured cells or frozen liver tissues were fractionated by cytoplasm lysis buffer (10mM HEPES, PH7.9; 10mM KCl; 0.1mM EDTA; 0.3% NP-40) and nucleus lysis buffer (20mM HEPES, PH7.9; 0.4M NaCl; 1mM EDTA; 25% Glycerol) (Zhou et al., 2010). Western blot analysis was performed, as described previously (Yang et al., 2013).

Metabolomics Analysis

Metabolomics analyses were performed at the West Coast Metabolomics Center, UC Davis (Fiehn O. et al. Plant J. 53 (2008) 691–704). Briefly, 50 mg frozen liver tissues from each mouse were used for gas chromatography/mass spectrometry (GC/MS). All gas chromatography analyses were performed with an Agilent 6890 gas chromatograph controlled using Leco ChromaTOF software version 2.32 and a 30 m long, 0.25 mm internal diameter Rtx-5Sil MS column with 0.25 lm 95% dimethyl/5% diphenyl polysiloxane film. A Leco Pegasus IV time-off light mass spectrometer was used with unit mass resolution at 17 spectra s-1 from 80-500 Da at -70 eV ionization energy and 1800 V detector voltage with a 230°C transfer line and a 250°C ion source. Leco ChromaTOF vs. 2.32 was used for data preprocessing. The actual data were given as peak heights and processed to a variant of a 'vector normalization' by calculating the sum of all peak heights for all identified metabolites and a subsequent normalization to the average mTIC of each group if necessary.

Mass Spectrometry (LC-MS) Analysis

Protein digests were analyzed using LC MS/MS on either a Waters/Micromass AB QSTAR Elite or a Thermo Scientific LTQ-Orbitrap XL mass spectrometer. Both systems are equipped with Waters nanoACQUITY ultra high pressure liquid chromatographs (UPLC) for peptide separation. The MS/MS spectra are searched in-house using the Mascot algorithm (Hirosawa et al, 1993) for un-interpreted MS/MS spectra after using the Mascot Distiller program to generate Mascot compatible files. The Mascot Distiller program combines sequential MS/MS scans from profile data that have the same precursor ion. A charge state of +2 and +3 are preferentially located with a signal to noise ratio of 1.2 or greater and a peak list is generated for database searching. Either the NCBInr, a species specific, or a custom database (in FASTA format) is used for searching. All Mascot search results are loaded into the Yale Protein Expression Database (YPED) online viewing system for dissemination to the investigator.

Score: The protein score in a Peptide Summary is derived from the ions scores. For a search that contains a small number of queries, the protein score is the sum of the unique ions scores. That is, excluding the scores for duplicate matches. A small correction is applied to reduce the contribution of low-scoring random matches. This correction is a function of the total number of molecular mass matches for each query and the width of the peptide tolerance window. This correction is usually very small, except in no enzyme searches https://medicine.yale.edu/keck/proteomics/yped/

Data availability

Additional supporting data are available upon request from the corresponding author.

References

Huang, J., Iqbal, J., Saha, P.K., Liu, J., Chan, L., Hussain, M.M., Moore, D.D., and Wang, L. (2007). Molecular characterization of the role of orphan receptor small heterodimer partner in development of fatty liver. Hepatology 46, 147-157.

Tabbi-Anneni, I., Cooksey, R., Gunda, V., Liu, S., Mueller, A., Song, G., McClain, D.A., and Wang, L. (2010). Overexpression of nuclear receptor SHP in adipose tissues affects diet-induced obesity and adaptive thermogenesis. American journal of physiology. Endocrinology and metabolism 298, E961-970.

Tsai, M.C., Manor, O., Wan, Y., Mosammaparast, N., Wang, J.K., Lan, F., Shi, Y., Segal, E., and Chang, H.Y. (2010). Long noncoding RNA as modular scaffold of histone modification complexes. Science 329, 689-693.

Venkatraman, A., He, X.C., Thorvaldsen, J.L., Sugimura, R., Perry, J.M., Tao, F., Zhao, M., Christenson, M.K., Sanchez, R., Yu, J.Y., Peng, L., Haug, J.S., Paulson, A., Li, H., Zhong, X.B., Clemens, T.L., Bartolomei, M.S., and Li, L. (2013). Maternal imprinting at the H19-Igf2 locus maintains adult haematopoietic stem cell quiescence. Nature 500, 345-349.

Wu, H., Ng, R., Chen, X., Steer, C.J., and Song, G. (2015). MicroRNA-21 is a potential link between non-alcoholic fatty liver disease and hepatocellular carcinoma via modulation of the HBP1-p53-Srebp1c pathway. Gut.

Yang, Z., Zhang, Y., and Wang, L. (2013). A feedback inhibition between miRNA-127 and TGFbeta/c-Jun cascade in HCC cell migration via MMP13. PloS one 8, e65256.

Zhang, L., Yang, Z., Trottier, J., Barbier, O., and Wang, L. (2017). Long noncoding RNA MEG3 induces cholestatic liver injury by interaction with PTBP1 to facilitate shp mRNA decay. Hepatology 65, 604-615.

Zhang, Y., Liu, C., Barbier, O., Smalling, R., Tsuchiya, H., Lee, S., Delker, D., Zou, A., Hagedorn, C.H., and Wang, L. (2016). Bcl2 is a critical regulator of bile acid homeostasis by dictating Shp and lncRNA H19 function. Scientific reports 6, 20559.

Zhang, Y., Xu, N., Xu, J., Kong, B., Copple, B., Guo, G.L., and Wang, L. (2014). E2F1 is a novel fibrogenic gene that regulates cholestatic liver fibrosis through the Egr-1/SHP/EID1 network. Hepatology 60, 919-930.

Zhou, T., Zhang, Y., Macchiarulo, A., Yang, Z., Cellanetti, M., Coto, E., Xu, P., Pellicciari, R., and Wang, L. (2010). Novel polymorphisms of nuclear receptor SHP associated with functional and structural changes. The Journal of biological chemistry 285, 24871-24881.

Supporting Table 1 Primers list

Primers*	Sequences (5' to 3')	
	Sense	anti-sense
hH19	TGGTGCACTTTACAACCACTG	ATGGTGTCTTTGATGTTGGGGC
hPTBP1	ATTGTCCCAGATATAGCCGTTG	GCTGTCATTTCCGTTTGCTG
hSREBF1	CACCAGCGTCTACCATAGC	AAAGAGAAGCACCAAGGAGAC
mAcc2	GCAGCTCCTATGCCTGGGTA	TGCAGCCTGTGTGCGATAG
mApoa1	GGCACGTATGGCAGCAAGAT	CCAAGGAGGAGGATTCAAACT
mApoa4	GAAGACGGATGTCACTCAGC	CTTCACCCTCTCAGTTTCCTG
mApoa5	TCCTCGCAGTGTTCGCAAG	CGAAGCTGCCTTTCAGGTTCT
mApob	TTGGCAAACTGCATAGCATCC	TCAAATTGGGACTCTCCTTTA
mApoc2	AAGACATACCCGATCAGCATG	AGGAGAGTAAGGAGCTGGTC
mApoc3	GCGTGCAGGAGTCCGATATAG	GAGTTGGTTGGTCCTCAGGGT
mApoe	CTGACAGGATGCCTAGCCG	CGCAGGTAATCCCAGAAGC
mCD36	GCGACATGATTAATGGCACAG	GATCCGAACACAGCGTAGATAG
mChREBP	TAGACAACAACAAGATGGAGAACCG	GCTGGGCTGGGCACTGAG
mCpt1	ACACCACATAGAGGCAGAAGAGG	CACAACAACGGCAGAGCAGAG
mEgr1	GACGAGTTATCCCAGCCAAA	GGCAGAGGAGACGATGAAG
mFasn	TCGGGTGTGGTGGGTTTGG	GCGTGAGATGTGTTGCTGAGG
mFxr	GTGAATGAGGACGACAGCGAAG	TGGTCTGCCGTGAGTTCCG
mG6pc	GGAAGGATGGAGGAAGGAATGAAC	TCAGCAATCACAGACACAAGGATG
mG6pd2	TATGTGAAGAATGAACGGTGGGATG	CGCCTGGTATATCTCGGAATTGC
mGk	CGGAGCAGAAGGGAACAACATC	TCATTCACCATTGCCACCACATC
mH19	GAACAGAAGCATTCTAGGCTG	TTCTAAGTGAATTACGGTGGG
mHgf	GATTATTGCCCTATTTCCCGTTGTG	CTACTGTTGTTTGTGTTGGAATGCC
mIrs1	CAGCAGCAGTAGCAGCATCAG	TACCGCCACCACTCTCAACAG
mIrs2	CCTCTACCACCACCGTCACC	GGCGGCTCATCACCTCCTC
mMtp	GCCTTGAACTTCCAACAAACCATAG	ATTACACCTGCCACTTGCTTCC
mNr1d1	TACATTGGCTCTAGTGGCTCC	CAGTAGGTGATGGTGGGAAGT
mPepck	ACAGAAGGGCGAGAGAACCAG	GGAAGGAAGGAGCATAGCAAAGC
mPk	GTGCCGCCTGGACATTGAC	TTCAGCCGAGCCACATTCATTC
mPparα	AGAGCCCCATCTGTCCTCTC	ACTGGTAGTCTGCAAAACCAA
mPparγ	CCACAGTTGATTTCTCCAGCATTTC	CAGGTTCTACTTTGATCGCACTTTG
mSrebf1	TTGCTGGCTTGGTGATGCTATG	CTGGTGGAGGGCTGGAAGG
T3	5'-ATTAACCCTCACTAAAGG-3'	
T7	5'AATACGACTCACTATAGG-3'	

*h: human; m: mouse

Supporting Table 2

PROTEIN ID	PROTEIN NAME	MW	% COVERAGE[1]	EMP AI[2]
PTBP1_MOUSE	Polypyrimidine tract-binding protein 1	56443	66.4	4.02
SGPL1_MOUSE	Sphingosine-1-phosphate lyase 1	63636	38	2.92
MCCB_MOUSE	Methylcrotonoyl-CoA carboxylase beta chain, mitochondrial	61340	50.3	2.14
SYFA_MOUSE	Phenylalanine--tRNA ligase alpha subunit	57563	49	2.39
HNRPK_MOUSE	Heterogeneous nuclear ribonucleoprotein K	50944	46	2.97
NONO_MOUSE	Non-POU domain-containing octamer-binding protein	54506	54.8	3.22
LAP2B_MOUSE	Lamina-associated polypeptide 2, isoforms beta/delta/epsilon/gamma	50342	50.7	2.71
YBOX1_MOUSE	Nuclease-sensitive element-binding protein 1	35709	49.4	1.82
SF3A3_MOUSE	Splicing factor 3A subunit 3	58805	35.3	1.32
DDX28_MOUSE	Probable ATP-dependent RNA helicase DDX28	59478	31.3	1.47
STAU1_MOUSE	Double-stranded RNA-binding protein Staufen homolog 1	53891	38.8	1.71
YBOX3_MOUSE	Y-box-binding protein 3	38790	45.2	1.34
PDIA1_MOUSE	Protein disulfide-isomerase	57023	24	0.92
PRS4_MOUSE	26S protease regulatory subunit 4	49154	24.3	0.66
IFRD1_MOUSE	Interferon-related developmental regulator 1	49903	17.8	0.64
PTBP3_MOUSE	Polypyrimidine tract-binding protein 3	56665	32.3	0.93
HBB1_MOUSE	Hemoglobin subunit beta-1	15830	44.9	2.6
TBA1A_MOUSE	Tubulin alpha-1A chain	50104	21.5	0.64
RBM42_MOUSE	RNA-binding protein 42	49844	28.3	0.79
PAIRB_MOUSE	Plasminogen activator inhibitor 1 RNA-binding protein	44687	33.2	0.91
RL4_MOUSE	60S ribosomal protein L4	47124	28.6	0.85
FA98A_MOUSE	Protein FAM98A	55021	22.7	0.46
HBA_MOUSE	Hemoglobin subunit alpha	15076	41.5	2.85
KPYM_MOUSE	Pyruvate kinase PKM	57808	31.1	0.54
DDX5_MOUSE	Probable ATP-dependent RNA helicase DDX5	69247	21.3	0.35
VIME_MOUSE	Vimentin	53655	21.7	0.72
HNRPQ_MOUSE	Heterogeneous nuclear ribonucleoprotein Q	69590	17.5	0.35
HNRPF_MOUSE	Heterogeneous nuclear ribonucleoprotein F	45701	18.8	0.2
TCPD_MOUSE	T-complex protein 1 subunit delta	58030	14.3	0.33
PLRG1_MOUSE	Pleiotropic regulator 1	56902	18.3	0.24
HNRH1_MOUSE	Heterogeneous nuclear ribonucleoprotein H	49168	12.2	0.18
ATPA_MOUSE	ATP synthase subunit alpha, mitochondrial	59716	13.7	0.23
ALBU_MOUSE	Serum albumin	68648	11.7	0.06
RTCB_MOUSE	tRNA-splicing ligase RtcB homolog	55214	24.4	0.45
RS27A_MOUSE	Ubiquitin-40S ribosomal protein S27a	17939	21.8	0.25
GIMA1_MOUSE	GTPase IMAP family member 1	30809	10.8	0.14
LECT1_MOUSE	Leukocyte cell-derived chemotaxin 1	37201	14.1	0.12

Supporting Table 2

ZFY27_MOUSE	Protrudin	46172	12.8	0.09
TBCA_MOUSE	Tubulin-specific chaperone A	12750	19.4	0.37
KCRU_MOUSE	Creatine kinase U-type, mitochondrial	46974	15.8	0.09
TMC6_MOUSE	Transmembrane channel-like protein 6	90487	10.6	0.05
ZMAT3_MOUSE	Zinc finger matrin-type protein 3	31981	11.4	0.14
NFS1_MOUSE	Cysteine desulfurase, mitochondrial	50538	11.1	0.09
RT17_MOUSE	28S ribosomal protein S17, mitochondrial	13373	26.7	0.36
TCPE_MOUSE	T-complex protein 1 subunit epsilon	59586	12.2	0.05
IQCAL_MOUSE	IQ and AAA domain-containing protein 1-like	95896	10.3	0.05
PDXK_MOUSE	Pyridoxal kinase SV=1	34993	11.9	0.12
PAI1_MOUSE	Plasminogen activator inhibitor 1	45141	10.2	0.1

1. Percent coverage indicates as to what percent of amino acids (of a particular protein) were covered.
2. Empai value estimates the protein abundance using the correlation between the number of identified peptides and protein abundance. Empai shows a high (0.89) correlation with the actual protein amount in complex mixtures of proteins.

Supporting Table 3. Clinical and biochemical characteristics of patients with non-alcoholic steatohepatitis (NASH).

Characteristics	**NASH-No-Fat (n=16)**	**NASH-Fat (n=20)**
Age (years)	57.2 ± 2.6	57.9 ± 1.8
Gender, male/female	7/9	6/14
MELD score	26.8 ± 2.1	30.2 ± 1.8
Total bilirubin (mg/L)	9.8 ± 3.2	13.8 ± 3.8
Creatinine (mg/L)	3.9 ± 0.7	2.1 ± 0.31*
Albumin (g/dL)	2.8 ± 0.14	3.0 ± 0.14
AST (U/L)	74.4 ± 14.9	66.4 ± 6.8
ALP (U/L)	225.5 ± 38.1	160.3 ± 20.9

Data are presented as means ± sem. MELD, model for end-stage liver disease; AST, aspartate transaminase, ALP; alkaline phosphatase. * $P<0.05$ *versus* NASH-No-Fat by Students unpaired t-test.

The human liver specimens were obtained through the Liver Tissue Cell Distribution System (LTCDS) (Minneapolis, Minnesota). NASH-No-Fat samples are defined as NASH (No longer Fatty) and NASH-Fat samples are defined as NASH (with Fatty Liver) per LTCDS.